

Adaptive EWMA Control Charts with Time-Varying Smoothing Parameter

Willy Ugaz*, Ismael Sánchez†, Andrés M. Alonso‡

Universidad Carlos III de Madrid

Abstract

Time-weighted charts like EWMA or CUSUM are designed to be optimal to detect a specific shift. This feature, however, can make the chart suboptimal for some other shifts. If, for instance, the charts are designed to detect a small shift, then, they can be inefficient to detect moderate or large shifts. In the literature, several alternatives have been proposed to circumvent this limitation, like the use of control charts with variable parameters or adaptive control charts. This paper aims to propose new adaptive EWMA control charts (AEWMA) based on the assessment of a potential misadjustment, which is translated into a time-varying smoothing parameter. The resulting control charts can be seen as a smooth combination between Shewhart and EWMA control charts, which could be efficient for a wide range of shifts. Markov chain procedures are established to analyse and design the proposed charts. Comparisons with other adaptive and traditional control charts show the advantages of our proposals.

Keywords: Adaptive control charts, Average Run Length , EWMA, CUSUM, Statistical Process Control, Misadjustment.

Accepted at International Journal of Advanced Manufacturing Technology

<https://doi.org/10.1007/s00170-017-0792-1>

**Address:* Willy Ugaz, Department of Statistics; Universidad Carlos III de Madrid; Avd. de la Universidad 30, 28911, Leganés, Madrid, Spain. email: wugaz@est-econ.uc3m.es.

†*Address:* Ismael Sánchez, Department of Statistics; Universidad Carlos III de Madrid; Avd. de la Universidad 30, 28911, Leganés, Madrid, Spain. And Department of Industrial Engineering and Systems; Universidad de Piura; Calle Ramón Mugica 131, Piura, Perú. email: ismael@est-econ.uc3m.es, ismael.sanchez@udep.pe.

‡*Address:* Andrés M. Alonso, Department of Statistics and IFL; Universidad Carlos III de Madrid; Calle Madrid 126, 28903, Getafe, Madrid, Spain. email: amalonso@est-econ.uc3m.es.

1 Introduction

Shewhart (1931), in studying the fundamentals of Statistical Process Control (SPC), supposed a change of paradigm in the concept of quality control, changing the focus from a control based on the verification of the final specifications to one based on the monitoring of the intrinsic variability of a process. Shewhart proposed charts based on monitoring the value of a statistic on independent samples, usually denoted as rational subgroups. These charts are known as Shewhart control charts. Let X be a random variable representing a quality characteristic of a product obtained from the process we want to monitor. Let us denote the mean and variance of X when the process is in control as μ_0 and σ^2 , respectively. Let $x_{i1}, x_{i2}, \dots, x_{in}$ be a set of realisations of X that conform the i -th rational subgroup of size n , being \bar{x}_i its sample mean. A Shewhart \bar{X} control chart monitors the evolution of the sequence of the independent sampling means \bar{x}_i with the aim of ensuring the process mean does not change. Under the assumption that \bar{X} is normal, the control limits of the Shewhart \bar{X} chart are

$$\mu_0 \pm 3\sigma/\sqrt{n}. \quad (1)$$

These limits correspond to a prediction interval for \bar{X} of coverage $1 - \alpha = 0.9973$. The chart triggers an alarm if a sample mean falls outside these limits. The probability of a false alarm is then $\alpha = 0.0027$. Similarly, there are Shewhart control charts for some other statistics, like sampling variances, standard deviations, coefficient of variations and so forth. The evaluation of a control chart is usually performed in terms of the average run length (ARL), which is the average number of independent samples required to signal a change for a particular shift. The best chart will be the one with the lowest ARL when the process is out of control, for a given ARL when the process is in-control, denoted as ARL_0 .

It is well known that \bar{X} control charts are not very sensitive to small shifts in the process mean. For example, it is easy to find out that if the shifted mean μ_1 is such that $|\mu_1 - \mu_0| < 2\sigma$, the probability of detecting such a change with the limits (1) is very small for practical purposes. In order to detect small shifts we need a statistics with lower variance that, for a given false alarm rate, can provide narrower control limits. This could be attained by using a larger subgroup size n . However, since Shewhart charts are based on independent samples, a larger rational subgroup size might lead to a larger average time to signal (ATS), or a larger average number of observations to signal (ANOS), apart from a higher cost. In order to increase the sensitivity of Shewhart control charts to smaller shifts, various studies have proposed the use of supplementary run rules. The run rules, initially proposed by Page (1955a), are a set of rules that help to detect when a sequence of points (i.e. a run) in a Shewhart control chart is very unlikely if the process were in control, even if the points are inside the control limits.

An alternative approach to improve the sensitivity of Shewhart control charts is by means of an adaptive design of the parameters; typically, variable sample sizes of the rational subgroups (VSS), variable sampling intervals (VSI) or some combination of both approaches. The main idea of this approach is to increase the sampling effort (larger size or higher frequency) only when data show some evidence of a shift. By doing so, we could take advantage of a larger information set without incurring a high cost. Basically, in a VSS chart, if the point falls in the so-called warning region, i.e. a region inside the control limits but close to them, the next sample size should be large to increase the sensitivity of the chart. However, if the point falls in the central region, the next sample size can be small, since there is no evidence that the process had shifted (Daudin, 1992; Prabhu et al., 1993, 1994; Costa, 1994; Zimmer et al., 1998; Wu, 2011; Zhang and Wang, 2012, and Castagliola et al., 2012). Similarly, in a VSI chart, the time to take the next sample should be smaller if the point falls in the warning region because the process could require a quick adjustment. Conversely, the time to take the next sample can be long if the current point falls in the central region, since the risk of being out of control is very low (Reynolds et al., 1988; Cui and Reynolds, 1988; Runger and Pignatiello, 1991; Costa, 1994, 1999a, 1999b; Tagaras, 1998; Mahadik, 2013).

An alternative procedure to reduce the variance of the monitoring statistics is to use a statistic with memory; that is, a statistics based on some average of current and past data, instead of a statistics based only on the last rational subgroup. By doing so, we are increasing the effective sample size, leading to a reduction in the sampling variability that would ease the detection of small shifts. These kinds of charts are denoted as time-weighted charts. These charts do not increase sampling costs; however, merging present and past observations in the same statistic can have a negative effect. If the process mean shifts, a monitoring statistic with memory would merge data corresponding to the shifted process with previous data, when the process was in control. This effect would bias the value of the statistics, masking the shift. This bias could provoke a delay in the detection. Therefore, if the shift is large, it might not be worthwhile to use a monitoring statistics with memory. Hence, time-weighted charts are competitive only in the case of small shifts. The decision of whether to use a Shewhart control chart or a memory control chart can then be interpreted as a particular case of the traditional bias-variance trade-off. Shewhart control charts have no bias, but large variance; whereas time-weighted charts have lower variance but estimate the shift with bias. The most popular time-weighted charts are CUSUM and EWMA charts. CUSUM control charts were introduced by Page (1954, 1955b) and then extended, among others, by Woodall and Adams (1993). The EWMA control chart was introduced by Roberts (1959) and subsequently studied by Robinson and Ho (1978), Hunter (1986), Waldmann (1986), Montgomery et al. (1987), Crowder (1987a and 1989) and Lucas

and Saccucci (1990), among others. The EWMA control chart is based on the statistic

$$y_t = \lambda x_t + (1 - \lambda) y_{t-1} = (1 - \lambda) y_0 + \lambda \sum_{i=0}^{t-1} (1 - \lambda)^i x_{t-i}, \quad (2)$$

where λ is a smoothing parameter such that $0 < \lambda \leq 1$, and $y_0 = \mu_0$. If $\lambda < 1$, the statistic (2) is an exponentially weighted average of current and past observations. The smaller the λ , the larger the weight to past data and, hence, the larger the effective sample size. Therefore, if we want to detect a small shift we would use a small value of λ . The variance of y_t for large values of t converges to

$$\sigma_y^2 = \frac{\sigma^2}{\frac{2-\lambda}{\lambda}} = \frac{\sigma^2}{M_{\text{eff}}}, \quad (3)$$

where, $M_{\text{eff}} = (2 - \lambda)/\lambda$ can be interpreted as the (asymptotic) effective number of observations or the effective memory length, which grows as λ decreases. The control limits of the EWMA chart for large t are then

$$\mu_0 \pm L\sigma \sqrt{\frac{\lambda}{2 - \lambda}}, \quad (4)$$

where L is a parameter that depends on the desired ARL. The optimal design of the EWMA charts depends on the value of λ . Once λ is selected, the chart would be optimal only for a specific shift. Similar comments also apply to CUSUM charts. With the aim of adding flexibility to CUSUM and EWMA charts, so that they perform well for either small or large shifts, VSI and VSS versions of these charts were proposed by Sawalapurkar et al. (1990), Reynolds et al. (1990), Baxley (1995), Keats et al. (1995), Reynolds (1995, 1996), Stoumbos and Reynolds (1996, 1997), Reynolds and Stoumbos (1998), Tagaras (1998), Reynolds and Arnolds (2001) and Arnolds and Reynolds (2001), among others.

Alternatively, adaptive time-weighted charts can be proposed based on time-varying versions of the parameters that control the length of memory of time-weighted charts. (Sparks, 2000; Capizzi and Masarotto, 2003). In the case of an adaptive EWMA (AEWMA), an appropriate time-varying parameter λ could make the chart sensitive to a large range of shifts.

Capizzi and Masarotto (2003) developed an AEWMA chart based on weighting recent observations using an appropriate function of the current error $e_t = x_t - y_{t-1}$. One goal of this weighting scheme is to diminish the so-called inertia problem of EWMA charts (Yashchin, 1987), which reduces the efficiency of the detection. If, for example, y_{t-1} is close to a control limit and x_t falls near the opposite control limit, the error e_t would be large. This large error would lead to a reduced value of λ , allowing the statistics to become closer to the new data quickly.

In this article, alternative AEWMA charts are proposed. The rationale behind the proposed adaptive charts is to make λ dependent on some measure of the potential presence of a shift. Accordingly, when the data show evidence of being affected by a large shift, the value of λ would tend to increase.

Conversely, if the data show evidence of being in control or, perhaps, being affected by a small shift, the value of λ would tend to be smaller.

The remainder of the article is organised as follows. In Section 2, the scheme of the proposed adaptive EWMA control chart is introduced. In Section 3, AEWMA control charts with time-varying λ based on the last observation x_t are proposed. In Section 4, AEWMA control charts with time varying λ based on the level of the control statistics y_{t-1} are proposed. Section 5 presents the results of several comparisons between alternative control charts and the proposed AEWMA control charts. Finally, in Section 6, some concluding remarks are given.

2 Adaptive EWMA strategy

The design of an EWMA chart consists of selecting the values of λ in (2) and L in (4). They can be chosen in such a way that the chart is optimal for detecting a prespecified shift $\delta\sigma$, such that the new mean is $\mu_1 = \mu_0 + \delta\sigma$. The optimisation of the design parameters of the EWMA chart was studied by Crowder (1987a, 1989) and Lucas and Saccucci (1990), among others. The optimal design can be based on approximating the ARL with a discrete Markov chain. The resulting ARL is a function of δ , λ and L ; that is, $ARL \equiv ARL(\delta, \lambda, L)$. The optimal values of λ and L that minimise $ARL(\lambda, L, \delta)$ for a given shift δ and ARL_0 can be obtained using traditional nonlinear optimisation procedures. This optimisation problem can be written as

$$\min_{\lambda, L} ARL(\lambda, L, \delta) \quad \text{subject to.} \quad ARL(\lambda, L, 0) = ARL_0.$$

Whereas an optimal EWMA chart needs a different value of λ for each δ , the same value of λ can be nearly optimal for some range of shifts. However, there is not a single value of λ that can provide optimal or nearly optimal EWMA charts for both small and large values of δ . To illustrate this finding, we have calculated the optimal pair (λ, L) denoted as (λ^*, L^*) for the values $\delta \in [0.1, 3]$ and $ARL_0 = 100$. The corresponding minimum ARL is denoted as ARL^* ; that is $ARL^* = ARL(\lambda^*, L^*, \delta)$. Figure 1 and Table 1 show the values of λ^* for each δ as well as the range of values of λ , denoted as the interval $[\lambda_a; \lambda_b]$, such that the corresponding ARL is not greater than a 5% of ARL^* ; that is, for $\lambda \in [\lambda_a; \lambda_b]$, then $ARL(\lambda, L, \delta) \leq 1.05ARL(\lambda^*, L^*, \delta)$. For instance, if $\delta = 1$ then it is possible to obtain an $ARL \in [6.96, 7.31]$ for $\lambda \in [0.0874, 0.3158]$. For example, if $\lambda = 0.10$, we obtain reasonable values of ARL for small shifts from $\delta \approx 0.5$ up to $\delta \approx 1$, but not for larger or smaller shifts. On the other hand, if we use, for instance, $\lambda = 0.5$, it is possible to obtain acceptable values of ARL for $\delta > 1.5$, but not for small shifts. Therefore, an EWMA chart with good performance for all shifts would need to adapt the value of λ to the expected shift.

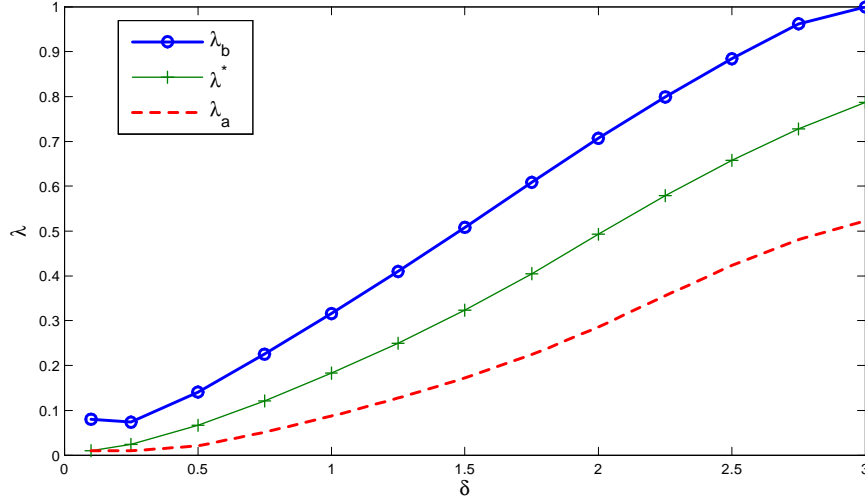


Figure 1: Relationship between the optimal λ and the range defined by λ_a and λ_b with the shift. The values λ_a and λ_b lead to an ARL of value $1.05ARL^*$.

δ	$ARL_0 = 100$				$ARL_0 = 500$			
	λ^*	ARL^*	$1.05ARL^*$	$\lambda_a - \lambda_b$	λ^*	ARL^*	$1.05ARL^*$	$\lambda_a - \lambda_b$
0.10	0.010	75.71	79.50	0.010-0.080	0.010	216.73	227.56	0.010-0.017
0.25	0.024	38.11	40.01	0.010-0.073	0.016	74.39	78.10	0.010-0.034
0.50	0.066	17.33	18.20	0.021-0.141	0.047	28.76	30.20	0.022-0.085
0.75	0.121	10.28	10.79	0.051-0.225	0.087	15.80	16.59	0.045-0.147
1.00	0.183	6.96	7.31	0.087-0.316	0.133	10.21	10.72	0.072-0.217
1.25	0.250	5.11	5.36	0.128-0.410	0.186	7.24	7.60	0.104-0.292
1.50	0.324	3.95	4.15	0.173-0.508	0.242	5.46	5.74	0.139-0.369
1.75	0.405	3.18	3.34	0.224-0.607	0.301	4.31	4.52	0.177-0.449
2.00	0.493	2.62	2.75	0.286-0.707	0.365	3.51	3.69	0.218-0.532
2.25	0.579	2.21	2.32	0.356-0.799	0.437	2.94	3.08	0.263-0.620
2.50	0.658	1.89	1.98	0.424-0.884	0.517	2.50	2.62	0.321-0.709
2.75	0.728	1.64	1.72	0.481-0.963	0.599	2.15	2.25	0.391-0.795
3.00	0.788	1.45	1.53	0.524-1.000	0.676	1.86	1.96	0.461-0.874

Table 1: ARL reached at each δ using the corresponding λ . ARL^* is reached using λ^* . $1.05ARL^*$ is reached using λ_a or λ_b

The goal of an AEWMA chart is to have a performance that is optimal or nearly optimal for any shift. Here, we will analyse alternative strategies to obtain AEWMA charts with time-varying smoothing parameters, using the representation

$$y_t = \lambda_t x_t + (1 - \lambda_t) y_{t-1}, \quad y_0 = \mu_0. \quad (5)$$

As shown above, this could be attained by making λ_t dependent on the shift. However, in practice, the shift is unknown (otherwise, we would trigger the alarm). Therefore it is necessary to find an alternative way of designing an adaptive EWMA chart. A natural option is to find a measure of the evidence of shift shown by the data, and translate that measure into an appropriate value λ_t . Conversely, if the data show little evidence of shifting, the parameter λ_t would be kept at a lower value. A small value of λ would increase the memory and, as a result, would keep the statistics with low variance, easing the detection of a potential small shift. Therefore, the parameter λ_t is used to manage the trade-off of having a control statistic y_t with low bias but high variance, or vice versa.

Three alternative measures of a potential shift are analysed: (i) based on the distance between the last observation x_t and the target μ_0 , (ii) based on the distance between the last observation x_t and the previous value of the control statistics y_{t-1} , following a similar fashion as in Capizzi and Masarotto (2003); and (iii) based only on the value of y_{t-1} . For each case, alternative score functions to translate each measure into a time-varying smoothing factor are also discussed. In each case, procedures to compute the ARL and to optimise the charts based on Markov chain approximations are proposed.

3 AEWMA charts with λ_t based on the last observation x_t

In this section, we present some proposals for λ_t as a function of the potential misadjustment based on the information provided by the last observation x_t . The first proposal, denoted as AEWMA1, is based on the standardised distance between x_t and the target μ_0 . The second proposal, denoted as AEWMA2, is based on the standardised distance between x_t and the last value of the monitoring statistics y_{t-1} . Finally, the third proposal is a combination of the two proposals above.

3.1 AEWMA1 chart

This adaptive control chart measures the potential misadjustment by standardising the last observation x_t . This is performed by using the following statistics:

$$S_{1t} = \left(\frac{x_t - \mu_0}{\sigma} \right)^2. \quad (6)$$

This distance tends to be larger in the presence of a shift, therefore it is an interesting measure of the potential misadjustment. We need now a transformation function that translates S_{1t} into a smoothing

factor. This function will be based on the statistical properties of S_{1t} . Given the information up to y_{t-1} , the value of x_t is a random variable. If the process is in control, and under the assumption of normality, it holds that S_{1t} follows a central chi-squared distribution of one degree of freedom, χ_1^2 . The cumulative distribution function is defined as

$$F_{1t} = P(\chi_1^2 \leq S_{1t}). \quad (7)$$

Note that $F_{1t} \in [0, 1]$ and, it tends to approach unity as the process departs from the in-control state. Therefore, it could be used as λ_t . However, the variability of F_{1t} can be very large, provoking a poor performance in the AEWMA chart. It should be noted that, according to (5), a large value of λ_t implies the loss of most of the memory accumulated in y_{t-1} , which can no longer be recovered, even if λ_t decreases in the following instants. This loss of memory would lead to a large variance of the monitoring statistic y_t , decreasing its sensitivity. We need, then, some efficient transformation that helps to translate F_{1t} into a smoothing parameter λ_t . Many transformations can be proposed. A simple transformation would be to limit the range of variation of F_{1t} , applying a linear transformation between a lower value λ_{\min} and an upper value λ_{\max} as follows:

$$\lambda_{1t}^{(1)} = \lambda_{\min} + (\lambda_{\max} - \lambda_{\min}) F_{1t}, \quad (8)$$

where, λ_{\min} and λ_{\max} are values that are optimised to attain the lowest ARL for a given ARL_0 , and computed with the procedure described below. A second alternative that adds some flexibility to the transformation (8) is to use also a power transformation as:

$$\lambda_{1t}^{(2)} = \lambda_{\min} + (\lambda_{\max} - \lambda_{\min}) F_{1t}^a, \quad (9)$$

where, a is a parameter to be optimised together with λ_{\min} and λ_{\max} . The third proposal to transform F_{1t} into λ_t is to use some threshold value, p_0 , such that if $F_{1t} \leq p_0$ then $\lambda_t = \lambda_{\min}$. Consequently, we will maintain a low smoothing factor unless the evidence of shift is large. If $F_{1t} > p_0$, we maintain a similar transformation as in (9) in such a way that the whole transformation is continuous. The resulting smoothing factor is

$$\begin{aligned} \lambda_{1t}^{(3)} &= \lambda_{\min} + (\lambda_{\max} - \lambda_{\min}) q_{1t}, \\ q_{1t} &= \begin{cases} 0 & \text{if } F_{1t}^a \leq p_0, \\ \frac{F_{1t}^a - p_0}{1 - p_0} & \text{otherwise,} \end{cases} \end{aligned} \quad (10)$$

where the threshold p_0 is a constant to be optimised together with a , λ_{\min} , and λ_{\max} . A fourth alternative, with further flexibility, is to fit the following polynomial:

$$\lambda_{1t}^{(4)} = \max(0, \min(1, r_{1t})), \quad (11)$$

$$r_{1t} = d + (b + cF_{1t})^a. \quad (12)$$

This fourth option also requires the optimisation of four parameters. In our experiments, option (10) is the one with better performance. Therefore, for the sake of conciseness, this transformation will be the only one that will be assumed hereafter, and labelled as the AEWMA1 chart. The chart triggers an alarm if $|y_t - \mu_0| > h_1\sigma$, where h_1 is a threshold that depends on the ARL_0 and is obtained in the same optimisation exercise as p_0 , a , λ_{\min} , and λ_{\max} .

3.2 AEWMA2 chart

This adaptive control chart measures the potential misadjustment by measuring the difference between the current observation x_t and the value of the control statistic in the previous time, y_{t-1} . This is carried out by using the following statistic:

$$S_{2t} = \left(\frac{x_t - y_{t-1}}{\sigma} \right)^2, \quad (13)$$

which, similar to the previous proposal, tends to increase in the presence of a shift. This statistic holds that

$$S_{2t} = \left(\frac{x_t - \mu_0}{\sigma} + \frac{\mu_0 - y_{t-1}}{\sigma} \right)^2. \quad (14)$$

Then, conditioning on y_{t-1} , S_{2t} follows a non-central chi-squared distribution of one degree of freedom, $\chi_1^2(\gamma_t)$, with noncentrality parameter $\gamma_t = (\mu_0 - y_{t-1})/\sigma$. As in the AEWMA1 chart, we could use the cumulative distribution function of $\chi_1^2(\gamma_t)$ to translate S_{2t} into a smoothing parameter, and then use the transformation (10) to obtain a time-varying smoothing parameter. It can be seen, however, that the noncentrality parameter γ_t can be very small. For instance, if $\lambda = 0.1$, expression (3) shows that y_{t-1} will have very small variability, $\sigma_{y_t}^2 \approx 0.05\sigma^2$. Consequently, y_{t-1} will be very close to μ_0 if we use as a unit of distance the standard deviation σ . Therefore, the order of magnitude of the noncentrality parameter γ_t will be very small for practical purposes. For the sake of simplicity, the conversion of S_{2t} into a smoothing factor will be performed as follows:

$$\begin{aligned} \lambda_{2t} &= \lambda_{\min} + (\lambda_{\max} - \lambda_{\min}) q_{2t}, \\ q_{2t} &= \begin{cases} 0 & \text{if } F_{2t}^a \leq p_0, \\ \frac{F_{2t}^a - p_0}{1 - p_0} & \text{otherwise,} \end{cases} \\ F_{2t} &= P(\chi_1^2 \leq S_{2t}). \end{aligned} \quad (15)$$

The chart triggers an alarm if $|y_t - \mu_0| > h_2\sigma$, where h_2 is a threshold that depends on the ARL_0 , and is obtained in the same optimisation exercise as p_0 , a , λ_{\min} , and λ_{\max} .

As explained above, since the variance of y_{t-1} is much smaller than that of x_t for small and moderate values of λ (i.e. those used in practice), the overall behaviour of S_{1t} and S_{2t} will not be dramatically different. However, we would expect some differences depending on the out-of-control situation. For instance, if a process is changing slowly, it can be expected that S_{1t} tends to take higher values than S_{2t} , because y_{t-1} will also tend to shift towards the new mean. As a result, both x_t and y_{t-1} would shift towards the same direction; consequently, their difference in (13) could not increase rapidly enough. In the case of an abrupt change, the behaviour of S_{1t} and S_{2t} depends on y_{t-1} . If it happens that y_{t-1} is close to a control limit and the sudden shift occurs in the opposite direction, S_{2t} will tend to be larger than S_{1t} . This situation is that described in the so-called "inertia problem" of EWMA charts, as explained in Yaschin (1987) and Capizzi and Masarotto (2003), among others. Conversely, if the shift is in the same direction as where y_{t-1} is located, S_{1t} would be more effective.

The AEWMA chart proposed by Capizzi and Masarotto (2003) is also based on $x_t - y_{t-1}$. They propose the statistic

$$y_t = w(e_t)x_t + (1 - w(e_t))y_{t-1}, ; \quad y_0 = \mu_0, \quad (16)$$

where, $e_t = x_t - y_{t-1}$, and $w(e_t)$ is some score function that translates e_t into a smoothing parameter monotonically non-decreasing in $|e|$. They propose three alternative score functions, but their performance is similar if their parameters are properly optimised.

3.3 AEWMA3 chart

Since both the AEWMA1 and AEWMA2 charts can be competitive depending on the specific situation, it would be interesting to propose a chart that could combine both approaches. This can be made in several ways. Since we want to take advantage of their different detection capabilities, we propose a chart, denoted as AEWMA3, which at each time computes both S_{1t} and S_{2t} , then compute S_{3t} as

$$S_{3t} = \max(S_{1t}, S_{2t}). \quad (17)$$

The conversion of S_{3t} into a smoothing factor λ_{3t} is performed just as in (15). The chart triggers an alarm if $|y_t - \mu_0| > h_3\sigma$, where h_3 is a threshold that depends on the ARL_0 and is optimised together with the parameters used in the computation of λ_{3t} . This AEWMA3 chart would tend to behave like AEWMA1 or AEWMA2, depending on which is more pessimistic with respect to the evidence of misadjustment.

4 AEWMA chart based on the value of the control statistics

In this AEWMA chart, denoted as AEWMA4, λ_t is based on the distance between y_{t-1} and the control limit $H = \mu_0 \pm h_4\sigma$, using the statistic

$$D_t = \left| \frac{y_{t-1} - \mu_0}{H - \mu_0} \right| = \left| \frac{y_{t-1} - \mu_0}{h_4\sigma} \right|,$$

which holds that $0 \leq D_t \leq 1$. In the same fashion as in previous proposals, the conversion of D_{tr} into a time-varying smoothing factor λ_{4t} is made by

$$\lambda_{4t} = \lambda_{\min} + (\lambda_{\max} - \lambda_{\min}) q_{4t}, \quad (18a)$$

$$q_{4t} = \begin{cases} 0 & \text{if } D_t^a \leq p_0, \\ \frac{D_t^a - p_0}{1 - p_0} & \text{otherwise.} \end{cases} \quad (18b)$$

As before, the chart triggers an alarm if $|y_t - \mu_0| > h_4\sigma$, where h_4 depends on the ARL_0 and is optimised together with the parameters λ_{\min} , λ_{\max} , p_0 and a shown in (18). Notice that, in this case, given y_{t-1} , the potential misadjustment, D_t , is deterministic.

5 Computation of ARL using a Markov chain approach

Similar to the Markov chain model suggested by Lucas and Saccucci (1990) or Capizzi and Masarotto (2003), we can approximate the value of ARL by discretising the infinite-state transition probability matrix of the continuous-state Markov chain defined by (5). For convenience, we rewrite the control statistics of the AEWMA as

$$y_t = y_{t-1} + (x_t - y_{t-1}) \lambda_t. \quad (19)$$

The procedure consists of dividing the interval between the upper and the lower control limits, of width $2h\sigma$, into an odd number $m_s = 2m + 1$ of subintervals Ω_j , $j = -m_s, -m_s + 1, \dots, m_s$, of width $\Delta = 2h\sigma/m_s$. The intervals Ω_j are then interpreted as states. The control statistic y_t is considered to be in the transient state Ω_j , at time t , if $\nu_j - \Delta/2 < y_t < \nu_j + \Delta/2$, where ν_j is the midpoint of the j th interval Ω_j . Furthermore, y_t falls in an absorbing state when it exceeds a threshold $H = \mu_0 + h\sigma$ or $-H$. The transition probability matrix between states can be represented in partitioned form as

$$\mathbf{P} = \begin{pmatrix} \mathbf{R} & (\mathbf{I} - \mathbf{R}) \mathbf{u} \\ \mathbf{0} & 1 \end{pmatrix}, \quad (20)$$

where \mathbf{R} is an $m_s \times m_s$ submatrix that contains the probabilities r_{jk} of going from the transient state j to the state k ; \mathbf{I} is the $m_s \times m_s$ identity matrix; and \mathbf{u} is an $m_s \times 1$ vector of ones. The elements of

the vector $(\mathbf{I} - \mathbf{R}) \mathbf{u}$ are the probabilities of jumping to the absorbing state from the transient state j . To approximate these probabilities, it is customary to assume that the statistic y_{t-1} is equal to ν_j whenever it is in state j . Therefore, using the form in (19), if $y_{t-1} \in \Omega_j$ we use the approximation $y_t = \nu_j + (x_t - \nu_j)\lambda_j$. The transition probability is then computed as

$$r_{jk} = \Pr(y_t \in \Omega_k \mid y_{t-1} \in \Omega_j) \quad (21a)$$

$$= \Pr(\nu_k - \Delta/2 < y_t \leq \nu_k + \Delta/2 \mid y_{t-1} = \nu_j) \quad (21b)$$

$$= \Pr\{\nu_k - \Delta/2 < \nu_j + (x_t - \nu_j)\lambda_t \leq \nu_k + \Delta/2\} \quad (21c)$$

$$= \Pr\{\nu_k - \nu_j - \Delta/2 < (x_t - \nu_j)\lambda_t \leq \nu_k - \nu_j + \Delta/2\}. \quad (21d)$$

In the next subsections we develop procedures to calculate r_{jk} for the AEWMA1 to AEWMA4 charts.

5.1 Computation of ARL of AEWMA1 to AEWMA3 charts

In the AEWMA1 to AEWMA3 charts, the time-varying smoothing parameter λ_t depends on x_t in a nonlinear way (e.g., (10)). Therefore, there is not an obvious way to solve for x_t in (21d). Besides, it is not trivial how the random term $(x_t - \nu_j)\lambda_t$ is distributed. Therefore, in order to compute (21d), we discretise x_t into $n_x = 2n + 1$ subintervals Ψ_i , $i = -n, -n + 1, \dots, n$. Since $x_t \sim N(\mu, \sigma^2)$, we first select a central interval of very high probability, and divide it into smaller intervals of equal width. Then, we add the two intervals at the tails. Accordingly, we divide the interval $\mu \pm 4.5\sigma$, into $2n - 1$ intervals Ψ_i , $i = -n + 1, -n + 2, \dots, n - 1$, of width $\varepsilon = 9\sigma/2n$, being u_i the midpoint of the i -th interval Ψ_i . If $x_t \in \Psi_i$ then $u_i - \varepsilon/2 < x_t \leq u_i + \varepsilon/2$. In each of these intervals, we approximate x_t to the value u_i . We then have two more intervals that are at the tails the distribution of x_t . The lower tail is the interval Ψ_{-n} . If $x_t \in \Psi_{-n}$ then $x_t \leq u_{-n+1} - \varepsilon/2$, and would approximate x_t to the value $u_{-n+1} - \varepsilon$. Similarly, the upper tail is the interval Ψ_n . If $x_t \in \Psi_n$ then $x_t > u_{n-1} + \varepsilon/2$, and would approximate x_t to the value $u_{n-1} + \varepsilon$. The approximate values of x_t can be used to assign an approximate value to λ_t in each interval according to the definition of λ_t in each AEWMA chart.

Regarding the AEWMA1 chart, if $x_t \in \Psi_i$, we can write

$$S_{1t} \approx \left(\frac{u_i - \mu_0}{\sigma} \right)^2 \equiv s_i. \quad (22)$$

Then,

$$\begin{aligned}
f_i &= P(\chi_1^2 < s_i), \\
q_i &= \begin{cases} 0 & \text{if } f_i \leq p_0, \\ \frac{f_i^a - p_0}{1 - p_0} & \text{otherwise,} \end{cases} \\
\lambda_i &= \lambda_{\min} + (\lambda_{\max} - \lambda_{\min}) q_i.
\end{aligned}$$

In order to compute r_{jk} in (21) we will condition on each interval Ψ_i , and apply the total probability theorem as

$$r_{jk} = \Pr(\nu_k - \nu_j - \Delta/2 \leq (x_t - \nu_j) \lambda_t \leq \nu_k - \nu_j + \Delta/2) \quad (23)$$

$$= \sum_{i=-n}^n \Pr(\nu_k - \nu_j - \Delta/2 \leq (x_t - \nu_j) \lambda_t \leq \nu_k - \nu_j + \Delta/2 \mid x_t \in \Psi_i) \Pr(x_t \in \Psi_i) \quad (24)$$

$$\approx \sum_{i=-n}^n \Pr(\nu_k - \nu_j - \Delta/2 \leq (u_i - \nu_j) \lambda_{(i)} \leq \nu_k - \nu_j + \Delta/2) \Pr(x_t \in \Psi_i) \quad (25)$$

$$= \sum_{i=-n}^n \Pr\left(v_j + \lambda_{(i)}^{-1}(\nu_k - \nu_j - \Delta/2) \leq u_i \leq v_j + \lambda_{(i)}^{-1}(\nu_k - \nu_j + \Delta/2)\right) \Pr(x_t \in \Psi_i) \quad (26)$$

Note that since u_i is a constant in each interval, the first probability in the right hand side of (26) is straightforward to compute, since it is just 1 or 0. The second is also easy to compute, since we assume that $x_t \sim N(\mu, \sigma^2)$. Once we obtain \mathbf{R} , we can compute three type of ARLs: (i) ARL_0 as the in-control ARL since the beginning of the monitoring, or since the monitoring is restarted after an alarm; (ii) ARL_1^{ZS} as the zero-state out-of-control ARL, which is the ARL if the process is already out-of-control when the monitoring starts; and (iii) ARL_1^{SS} as the steady-state out-of-control ARL, which is the ARL if the process is in control when the monitoring starts, and a step shift in the mean occurs at a later time such that the effect of the starting value becomes negligible. For a discussion between zero-state and steady-state ARLs, see Lucas and Saccucci (1990).

Given $x_t \sim N(\mu_0 + \delta\sigma, \sigma^2)$ and a set of parameters $\beta = (\lambda_{\min}, \lambda_{\max}, p_0, a, h)$, the zero-state ARL for the AEWMA1 chart is computed as

$$\text{ARL}_i^{ZS}(\delta, \beta) = \mathbf{p}'_0 (\mathbf{I} - \mathbf{R})^{-1} \mathbf{u}, \quad i = 0, 1, \quad (27)$$

where \mathbf{p}_0 is the initial probability vector. In the zero-state case, it is a vector of zeroes except for a one at position $(m_s + 1)/2$. If $\delta = 0$, we obtain ARL_0^{ZS} , and if $\delta > 0$, we obtain ARL_1^{ZS} . $\text{ARL}_1^{SS}(\delta, \beta)$ can be approximated using the approach of Lucas and Saccucci (1990), based on a cyclical steady-state probability vector that also uses \mathbf{R} .

The ARL for the AEWMA2 and AEWMA3 charts is computed using the same procedure, but

instead of S_{1t} in (22), we use S_{2t} or S_{3t} , respectively, defined as

$$S_{2t} \approx \left(\frac{u_i - v_j}{\sigma} \right)^2 \equiv s_i \quad \text{and} \quad S_{3t} \approx \max \left\{ \left(\frac{u_i - v_j}{\sigma} \right)^2, \left(\frac{u_i - \mu_0}{\sigma} \right)^2 \right\} \equiv s_i. \quad (28)$$

5.2 Computation of ARL of AEWMA4 chart

For the AEWMA4 chart, since λ_{4t} does not depend on x_t , expression (21d) is easier to handle. Solving for x_t in (21d) we obtain,

$$r_{jk} = \Pr \left(\frac{\nu_k - \nu_j - \Delta/2}{\lambda_t} - \nu_j \leq x_t \leq \frac{\nu_k - \nu_j + \Delta/2}{\lambda_t} - \nu_j \right),$$

which can be calculated assuming that $x_t \sim N(\mu, \sigma^2)$.

5.3 Optimisation of parameters

Let $\beta = (\lambda_{\min}, \lambda_{\max}, p_0, a, h)$ be the parameters that define the AEWMA chart, and let $ARL^{ZS}(\delta, \beta)$ denote the zero-state ARL of a scheme with parameters equal to β and shift δ , where $x_t \sim N(\mu_0 + \delta\sigma, \sigma^2)$. Let ARL_0^{ZS} be the in-control ARL. In order to evaluate the performance of an AEWMA chart in a set of shifts $\boldsymbol{\delta} = (\delta_1, \dots, \delta_k)$ we need to define a function $f(\beta, \boldsymbol{\delta}) : \mathbb{R}^k \rightarrow \mathbb{R}$, which summarises the overall performance of the chart along the alternative shifts $\boldsymbol{\delta}$. This function will be minimised when the optimal parameters β^* are used. That is, β^* is the solution of the following optimisation problem:

$$\min_{\beta} f(\beta, \boldsymbol{\delta}).$$

subject to: (29)

$$ARL^{ZS}(0, \beta) = ARL_0^{ZS},$$

A choice for $f(\beta, \boldsymbol{\delta})$ could be, for instance, $f(\beta, \boldsymbol{\delta}) = \sum_{i=1}^k ARL^{ZS}(\delta_i, \beta)$. Here, we use the weighted Euclidean distance

$$f(\beta, \boldsymbol{\delta}) = \sum_{i=1}^k \omega_i (ARL^{ZS}(\delta_i, \beta) - ARL^*(\delta_i))^2, \quad (30)$$

where $ARL^*(\delta_i)$ is the minimum ARL for shift δ_i attained using the optimal EWMA chart, as shown in Table 1. This function is simple and has good performance. Besides, it allows us to specialise the chart over some range of values in which we are more interested.

Table 2 shows the optimal values β^* for $ARL_0^{ZS} = 100$ and for $ARL_0^{ZS} = 500$ based on (29) and (30) with rational subgroup of size $n = 1$. For each value of ARL_0^{ZS} two different designs are proposed and compared. In the first, the optimisation (29) is based on the range of shifts $\delta \in [0.5, 4]$, where (30) uses higher weights on the extremes of this interval. By doing so, we want to assure good sensitivity to small shifts, without losing efficiency at large shifts. The resulting charts are denoted as AEWMA1-1,

β^*	ARL ₀ =100					ARL ₀ =500				
	λ_{\min}^*	λ_{\max}^*	a^*	p_0^*	h^*	λ_{\min}^*	λ_{\max}^*	a^*	p_0^*	h^*
<i>Panel A</i>										
AEWMA1-1	0.0542	0.1131	5.1709	0.9911	0.3231	0.0427	0.1155	7.7337	0.9963	0.3832
AEWMA2-1	0.0570	0.0968	12.760	0.9766	0.3336	0.0365	0.1065	7.5720	0.9977	0.3447
AEWMA3-1	0.0560	0.0968	6.2038	0.9878	0.3301	0.0356	0.1040	11.8925	0.9928	0.3425
AEWMA4-1	0.0749	0.3214	8.1296	0.9920	0.4027	0.0519	0.1519	9.5670	0.8759	0.4280
<i>Panel B</i>										
AEWMA1-2	0.1629	0.2514	9.9998	0.9421	0.7024	0.1253	0.2001	1.4180	0.9975	0.7550
AEWMA2-2	0.1705	0.2423	9.8870	0.9369	0.7194	0.1291	0.1956	14.9812	0.9409	0.7685
AEWMA3-2	0.1579	0.2429	7.5258	0.9682	0.6843	0.1355	0.2252	8.7293	0.9966	0.7832
AEWMA4-2	0.1896	0.2179	14.8801	0.9800	0.7590	0.0943	0.3034	9.9854	0.7347	0.6212

Table 2: Optimal parameters of the AEWMA control charts. Panel A: parameters optimised for the range $\delta \in [0.5; 4]$. Panel B: parameters optimised for the range $\delta \in [1; 4]$.

AEWMA2-1, AEWMA3-1 and AEWMA4-1, respectively. In the second design, the optimisation (29) is based on the range of shifts $\delta \in [1, 4]$, where (30) again uses higher weights on the extremes of this interval. In this case, we want to assure good performance at moderate and large shifts. The resulting charts are denoted as AEWMA1-2, AEWMA2-2, AEWMA3-2 and AEWMA4-2, respectively. For simplicity, and without any loss of generality, $\mu_0 = 0$ and $\sigma = 1$ is assumed.

6 Comparisons

The performance of the proposed AEWMA control charts is compared in terms of the zero-state ARL in the range of shifts $\delta \in [0, 3]$. Also, they are compared to some other charts like traditional EWMA charts, Shewhart charts, the AEWMA control charts of Capizzi and Masarotto (2003) and the ACUSUM of Jiang et al. (2008) control charts. The proposed AEWMA charts are based on the optimal parameters shown in Tables 2 and 3.

Table 3 summarises the results for $ARL_0 = 100$. This table displays the results of: 1) the proposed AEWMA charts; 2) two EWMA charts that were designed to be optimal for shifts $\delta = 1$, with $\lambda=0.183$ (EWMA-1) and $\delta = 2$ with $\lambda=0.493$ (EWMA-2) (see Table 1); 3) a Shewhart control chart with rational subgroup size $n = 1$ (Shewhart); and 4) the best two AEWMA designs of Capizzi and Masarotto (2003) based on the Huber score function. The first one, labelled CM-1, is obtained by minimising the ARL in the range $\delta \in [0.5, 5]$, and the second one, labelled CM-2, is obtained by minimising the ARL in the range $\delta \in [1, 5]$. The adaptive chart with the lowest ARL at each shift is displayed in bold.

Table 3 shows that for small shifts ($\delta \in [0.25; 0.5]$) the charts designed for small shifts, with names

	δ							
	0.25	0.50	0.75	1.00	1.50	2.00	2.50	3.00
AEWMA1-1	40.03	17.66	10.83	7.76	4.91	3.52	2.66	2.06
AEWMA2-1	40.07	17.60	10.77	7.71	4.89	3.55	2.72	2.15
AEWMA3-1	40.06	17.62	10.79	7.72	4.89	3.53	2.69	2.12
AEWMA4-1	40.08	17.35	10.47	7.44	4.74	3.53	2.84	2.41
AEWMA1-2	47.56	19.38	10.65	7.06	4.12	2.87	2.16	1.69
AEWMA2-2	47.84	19.46	10.65	7.04	4.11	2.87	2.17	1.72
AEWMA3-2	47.15	19.22	10.61	7.07	4.16	2.91	2.20	1.74
AEWMA4-2	47.21	19.26	10.52	6.96	4.10	2.95	2.34	1.98
EWMA-1	46.82	19.11	10.49	6.96	4.12	2.97	2.36	2.00
EWMA-2	62.84	28.64	14.52	8.53	4.12	2.62	1.93	1.55
Shewhart	80.83	49.99	29.09	17.33	7.09	3.54	2.13	1.51
CM-1	40.08	17.52	10.63	7.56	4.78	3.46	2.64	2.05
CM-2	47.81	19.53	10.63	7.00	4.09	2.89	2.23	1.80

Table 3: ARL comparison between competing control charts for $ARL_0 = 100$ and mean shift $\mu = \mu_0 + \delta\sigma$. The adaptive chart with the lowest ARL at each shift is shown in bold.

with the extension '-1', have a better performance than the respective charts designed for larger shifts, named with the extension '-2'. It is noticeable, however, that the relative gain of using charts for small shifts when the shift is indeed small is much larger than their relative loss when the shift is large. For large shifts, most adaptive charts are rather similar for practical purposes.

For very small shifts ($\delta = 0.25$) the best chart is the proposed AEWMA1-1. AEWMA2-1, AEWMA3-1, AEWMA4-1 and CM-1 are also at a very short distance. For small shifts ($\delta \in [0.5; 0.75]$), the best chart is the proposed AEWMA4-1. For moderate and large shifts ($\delta \geq 1$), charts with extension '-2' are better than those with extension '-1', with the exception of the EWMA charts. For $\delta = 1.0$, the best adaptive chart is the proposed AEWMA4-2, with an ARL equal to EWMA-1, which is the optimal one for this shift. For larger shifts, $\delta > 1$, the best overall performance of an adaptive chart is attained with the proposed AEWMA1-2, being surpassed only by the non-adaptive EWMA-2 and, for very large shifts ($\delta = 3$) by the Shewhart chart.

Table 4 summarises the results for $ARL_0 = 500$. This table shows the ARL profiles of: 1) the proposed AEWMA charts; 2) two alternative EWMA charts designed to obtain the minimum ARL values at shifts $\delta = 1$, with $\lambda = 0.133$ (EWMA-1), and $\delta = 2$ with $\lambda=0.365$ (EWMA-2) (see Table 1); 3) a Shewhart control chart with rational subgroup size $n = 1$ (Shewhart); 4) the two AEWMA designs of Capizzi and Masarotto (2003) also used for $ARL_0 = 100$; and 5) two ACUSUM charts of Jiang et al. (2008), optimised to detect mean shifts over the range $[0.5, 4]$ (J-1) and $[1, 5]$ (J-2).

As in the case with $ARL_0 = 100$, the charts that are designed to detect smaller shifts (with label '-1') show better performance for small shifts ($\delta = 0.25, 0.5$) than those designed for larger shifts (with

	δ							
	0.25	0.50	0.75	1.00	1.50	2.00	2.50	3.00
AEWMA1-1	84.97	29.50	16.95	11.80	7.27	5.13	3.78	2.80
AEWMA2-1	82.00	29.53	17.29	12.17	7.61	5.43	4.06	3.04
AEWMA3-1	82.70	29.80	17.43	12.24	7.57	5.30	3.85	2.80
AEWMA4-1	85.19	28.87	16.32	11.30	7.03	5.16	4.12	3.45
AEWMA1-2	126.55	35.28	16.69	10.40	5.80	3.96	2.94	2.28
AEWMA2-2	128.57	35.69	16.75	10.38	5.76	3.93	2.92	2.28
AEWMA3-2	128.53	35.66	16.69	10.33	5.76	3.98	3.01	2.37
AEWMA4-2	105.04	31.25	15.95	10.42	6.15	4.41	3.48	2.91
EWMA-1	121.21	34.23	16.30	10.21	5.78	4.08	3.19	2.65
EWMA-2	211.96	65.42	26.15	13.35	5.72	3.51	2.57	2.06
Shewhart	374.17	201.58	103.12	54.59	17.89	7.26	3.60	2.15
CM-1	86.41	29.91	17.11	11.88	7.27	5.06	3.65	2.64
CM-2	130.87	36.38	16.94	10.45	5.78	3.95	2.94	2.26
J-1	96.34	31.47	17.66	12.18	7.40	5.15	3.75	2.79
J-2	147.49	39.25	17.42	10.57	5.81	3.99	3.00	2.37

Table 4: ARL comparison between competing control charts for $ARL_0 = 500$ and mean shift $\mu = \mu_0 + \delta\sigma$. The adaptive chart with the lowest ARL at each shift is shown in bold.

label '2'). Again, the advantages of the latter in the case of large shifts are much smaller than those of the former for small shifts. That is, considering the full range of shifts $\delta \in [0.25, 3]$, the adaptive charts optimised for small shifts have a better overall performance. We wonder then whether many practitioners would find it more convenient to select an adaptive control chart that is optimised for small shifts.

For small shifts ($\delta \leq 0.5$), the best performance is attained by the proposed control charts. For $\delta = 0.25$, the best are AEWMA2-1 and AEWMA3-1, which is also very similar to the case with $ARL_0 = 100$. For $\delta = 0.5$, the best is AEWMA4-1. For $\delta = 0.75$, AEWMA4-1 and AEWMA4-2 have the best performance, together with the non-adaptive EWMA-1. This result is also very close to that observed in Table 3 with $ARL_0 = 100$. At $\delta \geq 1$, the relative performance of the adaptive control charts optimised for large shifts is superior. These charts behave in a very similar way, with differences in ARL between them, and with the optimal EWMA-1, of less than one unit. Overall, slightly better performance in this range is attained by AEWMA3-2 and AEWMA2-2.

As a general recommendation, we can conclude that better overall performance and adaptability can be attained by charts optimised for small shifts. If we are interested in very small shifts, we can use the AEWMA2-1 or AEWMA3-1 charts; otherwise, the use of AEWMA4-1 could be recommended for its overall performance.

7 Conclusions

We have presented a family of adaptive control charts for monitoring the mean of a process based on the use of a time varying smoothing parameter. This smoothing parameter tends to be larger when there is some evidence that the mean could be shifting, reducing the memory of the chart and easing the detection of the new mean. The resulting charts are efficient for a wide range of shifts, especially for small and very small shifts. It is only in these ranges where the differences in ARL among competing approaches become more noticeable; whereas for large shifts, the ARL of most charts is low and comparable for practical purposes. The proposed AEWMA charts are very easy to understand and implement.

7.0.1 Acknowledgements

Authors gratefully acknowledge the financial support received from the Spanish MEC, under grant ECO2012-38442 and ECO2015-66593.

References

- [1] Acosta-Mejia C. A. (2007). Two sets of runs rules for the \bar{X} chart. *Quality Engineering*, 19, pp. 129-136.
- [2] Antzoulakos D. L. and Rakitzis A. C. (2008). The revised m-of-k runs rule. *Quality Engineering*, 20, pp. 75-81.
- [3] Arnold, J. C. and Reynolds, M. R. (2001). CUSUM control charts with variable sample sizes and sampling intervals. *Journal of Quality Technology*, 33, pp. 66-81.
- [4] Baxley R. V. (1995). An application of variable sampling interval control chart. *Journal of Quality Technology*, 27, pp. 275-282.
- [5] Beaton A. E. and Tukey J. W. (1974). The fitting of power series, meaning polynomials, illustrated on Band-Spectroscopic data. *Technometrics*, 16, pp. 147-185.
- [6] Capizzi G. and Masarotto G. (2003). An adaptive exponentially weighted moving average control chart. *Technometrics*, 45, pp. 199-207.
- [7] Castagliola, P., Zhang, Y., Costa, A., and Maravelakis, P. (2012). The variable sample size \bar{X} chart with estimated parameters. *Quality and Reliability Engineering International*, 28, pp. 687-699.
- [8] Champ C. W. and Woodall W. H. (1987). Exact results for Shewhart control charts with supplementary runs rules. *Technometrics*, 29, pp. 393-399.
- [9] Costa A. F. (1994). \bar{X} charts with variable sample size. *Journal of Quality Technology*, 26, pp. 155-163.
- [10] Costa A. F. B. (1999a). Joint \bar{X} and R charts with variable sample sizes and sampling intervals. *Journal of Quality Technology*, 31, pp. 387-397.
- [11] Costa A. F. B. (1999b). \bar{X} charts with variable parameters. *Journal of Quality Technology*, 31, pp. 408-416.
- [12] Costa A. F. B. and Rahim M. A. (2006). A single EWMA chart for monitoring process mean and process variance. *Quality Technology & Quantitative Management*, 3, pp. 295-305.
- [13] Crowder S. V. (1987a). Average run lengths of exponentially weighted moving average control charts. *Journal of Quality Technology*, 19, pp. 161-164.

- [14] Crowder S. V. (1989). Design of exponentially weighted moving average schemes. *Journal of Quality Technology*, 21, pp. 155-162.
- [15] Cui R. Q. and Reynolds M. R. (1988). Chart with runs and variable sampling intervals. *Communications in Statistics-Simulation and Computation*, 17, pp. 1073-1093.
- [16] Daudin J. J. (1992). Double sampling \bar{X} charts. *Journal of Quality Technology*, 24, pp. 78-87.
- [17] Davis R. B. and Woodall W. H. (1988). Performance of the control chart trend rule under linear shift. *Journal of Quality Technology*, 20, pp. 260-262.
- [18] Davis R. B., Homer A. and Woodall W. H. (1990). Performance of the zone control chart. *Communications in Statistics-Theory and Methods*, 19, pp. 1581-1587.
- [19] Derman C. and Ross S. M. (1997). *Statistical aspects of quality control*. San Diego, CA: Academic Press.
- [20] Han D. and Tsung F. (2004). A generalized EWMA control chart and its comparison with the optimal EWMA, CUSUM and GLR schemes. *The Annals of Statistics*, 32, pp. 316-339.
- [21] Han D., Tsung F. and Li Y. (2007). A CUSUM chart with local signal amplification for detecting a range of unknown shifts. *International Journal of Reliability, Quality and Safety Engineering*, 14, pp. 81-97.
- [22] Hawkins D. M. (1992). A fast, accurate approximation of average run lengths of CUSUM control charts. *Journal of Quality Technology*, 24, pp. 37-43.
- [23] Hawkins D. M. (1993). Cumulative sum control charting: An underutilized SPC tool. *Quality Engineering*, 5, pp. 463-477.
- [24] Huber P. J. (1981). *Robust statistics*. New York: Wiley.
- [25] Hunter J. S. (1986). The exponentially weighted moving average. *Journal of Quality Technology* 18, pp. 203-210.
- [26] Jiang W., Shu L. and Apley D. W. (2008). Adaptive CUSUM procedures with EWMA-based shift estimators. *IIE Transactions*, 40, pp. 992-1003.
- [27] Keats J. B., Miskulin J. D. and Runger G. C. (1995). Statistical process control scheme design. *Journal of Quality Technology*, 27, pp. 214-225.

- [28] Khoo M. B. C. and Ariffin K. N. B. (2006). Two improved runs rules for the Shewhart control chart. *Quality Engineering*, 18, pp. 173-178.
- [29] Klein M. (2000). Two alternatives to the Shewhart \bar{X} control chart. *Journal of Quality Technology*, 32, pp. 427-431.
- [30] Koutras M. V., Bersimis S. and Maravelakis P. E. (2007). Statistical process control using Shewhart control charts with supplementary runs rules. *Methodology and Computing in Applied Probability*, 9, pp. 207-224.
- [31] Lucas J. M. and Saccucci M. S. (1990). Exponentially weighted moving average control schemes: Properties and Enhancements (with discussion), *Technometrics*, 32, pp. 1-29.
- [32] Mahadik S. B. (2013). \bar{X} Charts with variable sample size, sampling interval, and warning limits. *Quality and Reliability Engineering International*, 29, pp. 535-544.
- [33] Montgomery D. C., Gardiner J. S. and Pizzano B. A. (1987). Statistical process control methods for detecting small process shifts. In *Frontiers in Statistical Quality Control*, eds. H.-J. Lenz, G. B. Wetherill, and P. T. Wilrich, Heidelberg, West Germany: Physica-Verlag, pp. 161-178.
- [34] Nelson C. S. (1984). The Shewhart control charts - test for special causes. *Journal of Quality Technology*, 16, pp. 237-239.
- [35] Page E. S. (1954). Continuous inspection schemes. *Biometrika*, 41, pp. 100-114.
- [36] Page E. S. (1955a). Control charts with warning lines. *Biometrika*, 42, pp. 243-257.
- [37] Page E. S. (1955b). A test for a change in a parameter occurring at an unknown point. *Biometrika*, 42, pp. 523-527.
- [38] Prabhu S. S., Runger G. C. and Keats J. B. (1993). \bar{X} chart with adaptive sample sizes. *The International Journal of Production Research*, 31, pp. 2895-2909.
- [39] Prabhu S. S., Montgomery D. C. and Runger G. C. (1994). A combined adaptive sample size and sampling interval \bar{X} control scheme. *Journal of Quality Technology*, 26, pp. 164-176.
- [40] Reynolds J. H. (1971). The run sum control chart procedure. *Journal of Quality Technology*, 3, pp. 23-27.
- [41] Reynolds M. R. (1995). Evaluating properties of variable sampling interval control charts. *Sequential Analysis*, 14, pp. 59-97.

- [42] Reynolds M. R. (1996a). Shewhart and EWMA variable sampling interval control charts with sampling at fixed times. *Journal of Quality Tecnology*, 28, pp. 199-212.
- [43] Reynolds M. R. (1996b). Variable-sampling-interval control charts with sampling at fixed times. *IIE transactions*, 28, pp. 497-510.
- [44] Reynolds, M. R., and Arnold, J. C. (2001). EWMA control charts with variable sample sizes and variable sampling intervals. *IIE transactions*, 33, pp. 511-530.
- [45] Reynolds, M. R., and Stoumbos, Z. G. (1998). The SPRT chart for monitoring a proportion. *IIE transactions*, 30, pp. 545-561.
- [46] Reynolds M. R, Amin R. W., Arnold J. C. and Nachlas J. A. (1988). \bar{X} Charts with Variable Sampling Intervals. *Technometrics*, 30, pp. 181-192.
- [47] Reynolds M. R., Amin R. W. and Arnold J. C. (1990). CUSUM charts with variable sampling intervals. *Technometrics*, 32, pp. 371-384.
- [48] Roberts S. W. (1959). Control chart tests based on geometric moving averages. *Technometrics*, 1, pp. 239-250.
- [49] Robinson P. B. and Ho T. Y. (1978). Average run lengths of geometric moving averages by numerical methods. *Technometrics*, 20, pp. 85-93.
- [50] Runger G. C. and Pignatiello J. J. (1991). Adaptive sampling for process control. *Journal of Quality Technology*, 23, pp. 135-155.
- [51] Sawalapurkar-Powers U., Arnold J. C. and Reynolds M. R. (1990). Variable sample size control charts. In the Annual Meeting of the American Statistical Association, Orlando, FL.
- [52] Shewhart W. A. (1931). *Economic control of quality of manufactured product*. D. Van Nostrand Company, Inc, The United States of America, pp. 182.
- [53] Shu L. (2008). An adaptive exponentially weighted moving average control chart for monitoring process variances. *Journal of Statistical Computation and Simulation*, 78, pp. 367-384.
- [54] Shu L. and Jiang W. (2006). A Markov chain model for the adaptive CUSUM control chart. *Journal of Quality Technology*, 38, pp. 135-147.
- [55] Shu L., Jiang W. and Wu Z. (2008). Adaptive CUSUM procedures with Markovian mean estimation. *Computational Statistics & Data Analysis*, 52, pp. 4395-4409.

- [56] Sparks R. (2000). CUSUM charts for signaling varying location shifts. *Journal of Quality Technology*, 32, pp. 157-171.
- [57] Steiner S. H. (1999). Exponentially weighted moving average control charts with time varying control limits and fast initial response. *Journal of Quality Technology*, 31, pp. 75-86.
- [58] Stoumbos Z. G. and Reynolds M. R. (1996). Control charts applying a general sequential test at each sampling point. *Sequential Analysis*, 15, pp. 159-183.
- [59] Stoumbos Z. G. and Reynolds M. R. (1997). Corrected diffusion theory approximations in evaluating properties of SPRT charts for monitoring a process mean. *Proceedings of the 2nd World Congress of Nonlinear Analysts*, 30, pp. 3987-3996.
- [60] Tagaras G. (1998). A survey of recent developments in the design of adaptive control charts. *Journal of Quality Technology*, 30, pp. 212-231.
- [61] Vance L. C. (1986). Average run lengths of cumulative sum control charts for controlling normal means. *Journal of Quality Technology*, 18, pp. 189-193.
- [62] Waldmann K. H. (1986). Bounds for the distribution of the run length of geometric moving average charts. *Journal of the Royal Statistical Society. Series C (Applied Statistics)*. 35, pp. 151-158.
- [63] Western Electric (1956). *Statistical quality control handbook*. Western Electric Corporation, Indianapolis, Ind.
- [64] Woodall W. H. and Adams B. M. (1993). The statistical design of CUSUM charts. *Quality Engineering*, 5, pp. 559-570.
- [65] Yashchin, E. (1987). Some aspects of the theory of statistical control schemes. *IBM Journal of Research and Development*, 31, pp. 199-205.
- [66] Wu, S. (2011). Optimal inspection policy for three-state systems monitored by variable sample size control charts. *The International Journal of Advanced Manufacturing Technology*, 55, pp. 689-697.
- [67] Zhang, J., Li, Z., and Wang, Z. (2012). A new adaptive control chart for monitoring process mean and variability. *The International Journal of Advanced Manufacturing Technology*, 60, pp. 1031-1038.

- [68] Zimmer L.S., Montgomery D.C and Runger G.C. (1998). Evaluation of a three-state adaptive sample size \bar{X} control chart. International Journal of Production Research, 36, pp. 733-743.